Copyright 2010, ABRACO
Trabalho apresentado durante o INTERCORR 2010, em Fortaleza/CE no mês de maio de 2010.
As informações e opiniões contidas neste trabalho são de exclusiva responsabilidade do(s) autor(es).

Electrochemical impedance spectroscopy as a technique for characterization of the oxide film formed on nickel alloy 52 at 325 °C

Célia A. Figueiredo[1], Rik-Wouter Bosch [2]

Abstract

Stress corrosion cracking (SCC) is a major concern in the plant life management of ageing plants. The main classes of nuclear power plant materials, that are potentially subjected to SCC, are austenitic stainless steels and nickel base alloys. The nickel alloys 600, 82 and 182 show, after many years of plant operation, susceptibility to SCC. Those alloys are used in steam generators and as dissimilar metal weld materials for nozzles of components such as the reactor pressure vessel and the pressurizer. The long-term exposure of Ni-based alloys in Pressurized Water Reactor (PWR) primary water leads to the development of an oxide corrosion film which is generally considered to influence the SCC behavior of the alloys. The structure, composition and thickness of the film depend on the chemical composition of the alloy and the exposure conditions. The nickel alloy 52, which is used in weld repair, was exposed to simulated PWR chemistry and the electrochemical behavior of the material was investigated by electrochemical impedance spectroscopy (EIS). The in-situ EIS measurements allowed monitoring of the oxide layer formation/change. Under PWR relevant conditions alloy 52 showed an increased resistance with time. With dissolved hydrogen the oxide layer resistance was smaller than without hydrogen. The experimental data were fitted to an equivalent circuit model to help understanding the corrosion behavior.

Key-words: impedance, nickel, oxide, PWR.

Introduction

Stress Corrosion Cracking (SCC) is a major concern in the plant life management of ageing plants. It occurs due to a combination of high temperature, stress and a susceptible material – environment combination. SCC is among others reflected by electrochemical processes that take place at the metal - oxide - solution interface.

The main classes of structural materials, applied in nuclear power plants, that are potentially subject to SCC, are austenitic stainless steels and nickel base alloys. It is generally recognized that the nucleation and propagation of localized corrosion and stress corrosion in particular is strongly related to the properties of the oxide film formed on the metal surfaces (1).

The oxide film formed on metallic materials in high temperature and high pressure water can be characterized using surface and microscopic analysis techniques after exposure. That

[1] PhD, Senior Researcher – CDTN/CNEN
[2] PhD, Senior Researcher – SCK.CEN (Bélgica)

means that the analysis is done ex-situ. It should be noted that the corrosion of metals and alloys in high temperature aqueous environments is an electrochemical process in nature. Therefore, it is possible to investigate the electrochemical behavior of the materials and the property of the oxide film in high temperature aqueous environments by electrochemical techniques (1). These techniques are in-situ i.e. the measurements are carried out during exposure of the specimens to the test environment.

In this paper the nickel alloy 52 was exposed to simulated Pressurized Water Reactor (PWR) chemistry and the electrochemical behavior of the oxide film was investigated by electrochemical impedance spectroscopy (EIS).

Evaluation of Impedance Data

The measured impedance data are commonly analyzed by fitting them to an equivalent electrical circuit model. Most of the circuit elements in the model are common electrical elements such as resistors, capacitors, and inductors.

Capacitors in EIS experiments often do not behave ideally. Instead, they act like a constant phase element. The impedance of a phase element is defined as $Z_{CPE} = 1/ [Y_o (j\omega)^n]$, where Y_o is the CPE coefficient = "capacitance", j is the imaginary unit, ω is the angular frequency ($=2\pi f$) and n the CPE exponent. The value of n is associated with the non-uniform distribution of current as a result of roughness and surface defects. When $n = 1$ it represents a capacitor.

The equivalent circuit used in the present work is shown in Figure 1. It consists of the electrolyte resistance, R_s, in series with a parallel circuit of a charge transfer resistance (R_1) and a constant phase element (Q_1), which is used to account for the process occurring at higher frequencies in the condition without hydrogen and for the process occurring at intermediate frequencies in the condition with 25 cm^3/kg H_2. Another parallel circuit consisting of charge transfer resistance (R_2) and the constant phase element (Q_2) was added to account for the process occurring at lower frequencies in both conditions (without H_2 and with 25 cm^3/kg H_2). The two time constants are related to different electrochemical phenomena, most probably separating the electrochemical behavior of the oxide layer and the solution interface. The commercial software ZSimpWin was used for the equivalent circuit analysis.

Experimental

Material

The samples used in this work were made of nickel alloy 52, which in this case was available as a wire shaped welding consumable. The chemical composition of this alloy 52 is shown in Table 1.

The alloy 52 wire (length: 5 m) was deposited on a plate of inconel 600 by the Gas Tungsten Arc Welding (GTAW) technique. Seven passes were made resulting in a small block of 5.5 cm^3, shown in Figure 2. Table 2 presents the conditions used to make the weld.

Four cylindrical specimens were cut from the block for the electrochemical tests. A piece of the weld was cut for metallurgical evaluation. It was embedded in resin and abraded with wet

SiC paper of decreasing grit size (180-320-600-1200-4000) followed by polishing with diamond pastes (3 µm and 1 µm). The polished surface was etched with Marble solution (50 % HCl + $CuSO_4$). Figure 3 shows the embedded surface and its microstructure. The dendritic microstructure is clearly visible.

Test set-up

The cylindrical specimens were exposed to PWR environment (1000 ppm B, 2 ppm Li, O_2 < 10 ppb) in the circulating autoclave shown in Figure 4. Two different conditions were tested: with and without dissolved hydrogen. The dissolved hydrogen concentration was 25 cm/kg H_2 under standard conditions, which was obtained by varying the hydrogen overpressure in the tank. For the condition without hydrogen, an overpressure of nitrogen gas was used in the tank. The temperature was 325 °C. The specimens were exposed for about one month under the two different dissolved hydrogen concentrations. Figure 5 shows the set-up for the electrochemical tests. The cylindrical specimens were connected to mineral insulated cables to electrically isolate them from the autoclave.

Impedance measurements

The impedance measurements were performed at the open circuit potential using a frequency range from 100 kHz to 1 mHz or from 100 kHz to 10 mHz (10 points per decade) with a perturbation amplitude of 10 mV RMS. The reference electrode was an yttrium stabilized zirconia type (YSZ) electrode and the counter electrode was the body of the autoclave. The measurements were performed once per day with a GAMRY® potentiostat system (PC4-300).

Results and Discussion

It was observed that the Nyquist curves under 0 hydrogen shifted to the left and to the right under 25 cm^3/kg H_2, with time of exposure, as shown in Figures 6 and 7. This behavior is related to the changing in the solution resistance during the exposure. To better visualize the effect of the exposure time , the impedance curves were superimposed on each other. Figure 8 and 9 show impedance data in two types of plots: Nyquist or complex plane plot and Bode plots (phase and magnitude) for the tests in PWR water without hydrogen and with 25 cm^3/kg H_2.

In the absence of H_2, the Bode diagram shows two time constants, one at high frequencies (~100 kHz) and the other at low frequency (10 mHz), each one assigned to a different electrochemical process occurring at the surface. A higher impedance is seen in the Nyquist diagram for the process at low frequency time constant than for the process at high frequency time constant. Similar results were also observed in other works. Park et al. (2) and Kim et al. (3) observed two capacitive loops from the impedance spectrum obtained for anodic films on Alloy 600 in the temperature range of (100–300) ºC. In addition, Carranza and Alvarez (4) also observed two well-defined phase angle maxima obtained on Alloy 800 in 0.1 $mol.L^{-1}$ NaCl solution at the temperature above 125 ºC. Those results correlate well with the well-known duplex structure of oxide films formed on Ni–Cr–Fe alloys in high temperature aqueous solutions (5, 6, 7). Kim et al. (3) consider that the high frequency arc is related to the outer and porous oxide layer having a low resistance while the low frequency arc is related to the inner, protective oxide layer having a relatively high resistance.

From the Nyquist diagram, it can be seen that there is an increase of the impedance at low frequencies from the first to the seventh day of exposure, decreasing afterwards to increase again until the end of the exposure. This behavior is explained by an interruption of the test for about 30 h in the first week of exposure due to a failure in the autoclave heating element. The maximum at high frequency in Bode plot, which is being associated with the outer layer, falls outside the measured frequency range. The reason for this is a low resistance together with a small capacitance. It can also be seen that the impedance decreases with time of exposure, probably due to electrolyte penetration. The electrolyte impedance influences the measurement at high frequencies (8).

In the presence of H_2, the Nyquist diagram shows two semicircles, one at intermediate frequencies (50 Hz -100 Hz) and the other at low frequencies (10 mHz) and the beginning of a third one at high frequencies (~ 100 kHz). The Bode plot shows three time constants related to three different electrochemical processes. The process occurring at low frequencies has higher impedance than the one occurring at intermediate frequencies. The time constant at intermediate frequencies is not present when H_2 is absent. So the presence of hydrogen influenced the onset of this intermediate time constant. Its phase and impedance decrease with time, so the resistance for this process decreases with time. In this work, this intermediate time constant is assumed to be associated to electrochemical reactions with hydrogen at the interface oxide-electrolyte.

At low frequencies, Figure 9 shows that the semicircles do not finish and the impedance values increase with time, reaching saturation after ca. 3 weeks of exposure. This behavior is related to mass transport processes in the oxide. It probably occurs due to the increase of film thickness, which makes the transport processes through the oxide film more difficult. The time constant at higher frequency would be associated with the porous outer oxide layer. The impedance associated to this time constant increases slightly with time.

The Bode plots presented phase angle maxima smaller than 90º at both investigated dissolved hydrogen conditions. Moreover, the Nyquist plots showed depressed semi-circles. Many reasons have been proposed in the literature to explain this behavior such as surface roughness, frequency dispersion of time constants due to local inhomogeneities in the dielectric material, porosity mass transport effects and relaxation effects (4). In order to account for these effects, a constant phase element (CPE) was introduced into the equivalent circuit proposed to reproduce the experimental results (Figure 1). In this figure, it is considered that the pairs (R_1, Q_1) and (R_2, Q_2) represent the charge transfer resistance and the capacitance associated to the electrochemical reactions at the interface oxide-electrolyte and the charge transfer resistance and the capacitance of the oxide film, respectively. A good agreement of the data to the proposed equivalent circuits was observed (shown in Figures 8 and 9).

From the equivalent circuit analysis the evolution with time of the parameters related to the oxide film (pair R2, Q2) for the two dissolved hydrogen conditions was evaluated, as shown in Figure 10. There is an increase in the pseudo-capacitance Y_o with time of exposure for both H_2 conditions. At 10 days of exposure there is a sharp increase of Y_o for the condition without hydrogen. We don´t see a correlation between the trend of the CPE exponent *n* and Y_o. This parameter stays approximately constant for the condition without hydrogen. Under 25 cm^3/kg H_2, *n* shows an increase during the first week and an approximately constant value afterwards.

After the fourth day of exposure the resistance drops for the condition without hydrogen. This behavior can be the result of the test interruption due to the heating element failure, which affected the oxide film growth. The resistance increases again in the last week of exposure. Under 25 cm^3/kg H_2, the resistance shows a continuous increase along the exposure time.

The presence of hydrogen was deleterious for the corrosion resistance of the alloy, according to equivalent circuit analysis. Figure 10c shows that the resistance of the oxide was lower under the condition with dissolved hydrogen but increased with time getting close to the resistance values of the condition without hydrogen. The experimental impedance data at low frequency (10 mHz) in Figure 11 show similar behavior. This behavior was also observed by Laitinen et al. (9) who studied the electrochemical properties of surface films forming on Cr, Fe, Ni, Alloy 600 and Alloy 690 in PWR water at 320 ^oC both in the presence and absence of dissolved hydrogen. In the case of Alloy 690, the removal of hydrogen resulted in a small increase of the film resistance. Alloys 690 and 52 have similar chemical composition.

Conclusions

In this work the electrochemical behavior of the nickel alloy 52 in simulated PWR primary water with different hydrogen concentrations was studied. Electrochemical impedance spectroscopy (EIS) was used to study the formation and growth of oxide films in-situ on the surface of the exposed samples.

The in-situ EIS measurements allowed monitoring of the oxide layer formation/change. The results showed that two time constants were present in the absence of H_2 and three time constants were present with 25 cm^3/kg H_2. In this work, no chemical composition analysis of the oxide film was performed but, based on literature data, it was concluded that the time constant at lower frequencies is related to the protective oxide film formed on the sample surface.

The data were fitted to an equivalent circuit model for the conditions with and without dissolved hydrogen. Under PWR relevant conditions alloy 52 showed an increased resistance with exposure time. When dissolved hydrogen is present there is a decrease in the oxide resistance.

References

1. SUN, H.; WU, X.; HAN, E-H. Effects of temperature on the protective property, structure and composition of the oxide film on Alloy 625. **Corrosion Science**, v. 51, p. 2565-2572, 2009.

2. PARK, J.-J.; PYUN, S.-I.; LEE, S.-B. Growth kinetics of passivating oxide film of Inconel alloy 600 in M Na_2SO_4 solution at 25–300◦C using the abrading electrode technique and ac impedance spectroscopy. **Electrochimica Acta**, v. 49, p. 281-292, 2004.

3. KIM, D.-J.; KWON, H.-C.; KIM, H.P. Effects of the solution temperature and the pH on the electrochemical properties of the surface oxide films formed on Alloy 600**. Corrosion Science**, v. 50, p. 1221-1227, 2008.

4. CARRANZA, R.M.; ALVAREZ, M.G. The effect of temperature on the passive film properties and pitting behaviour of a Fe-Cr-Ni alloy. **Corrosion Science**, v. 38, n. 6, p. 909–925, 1996.

5. SUN, M.C.; WU, X.Q.; ZHANG, Z.E.; HAN, E.H. **J. Supercrit. Fluids**, v. 47, p. 309–317, 2008.

6. MACHET, A.; GALTAYRIES, A.; ZANNA, S.; KLEIN, L.; MAURICE, V.; JOLIVET, P.; FOUCAULT, M; COMBRADE, P.; SCOTT, P.; MARCUS, P. XPS and STM study of the growth and structure of passive films in high temperature water on a nickel-base alloy. **Electrochimica. Acta**, v. 49, p. 3957–3964, 2004.

7. ROBERTSON, J. **Corrosion Science**, v. 32, p. 443–465, 1991.

8. FORSBERG, S.; AHLBER, E.; LIMBÄCK, M. Studies of corrosion of cladding materials in simulated BWR environment using impedance measurements. **Journal of ASTM International**, v. 4, n. 9, paper ID JAI101123, 2007.

9. LAITINEN, T.; MÄKELÄ, K.; SAARIO, T.; BOJINOV, M. Oxide films in high temperature aqueous environments. In: SOLIN, J.; SARKIMO, M.; ASIKAINEN, M.; ÅVALL, Å. (Ed.). RATU2 THE FINNISH RESEARCH PROGRAMME ON THE STRUCTURAL INTEGRITY OF NUCLEAR POWER PLANTS SYNTHESIS OF ACHIEVEMENTS 1995-1998. Espoo: VTT Manufacturing Technology, 1998. p. 145-166.

Acknowledgments

To CAPES, for the post doc fellowship, to SCK.CEN, to allow the development of this work and to FAPEMIG, for the sponsorship to present this work.

* * *

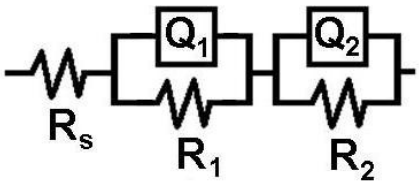

Figure 1. Equivalent circuit used to fit the data.

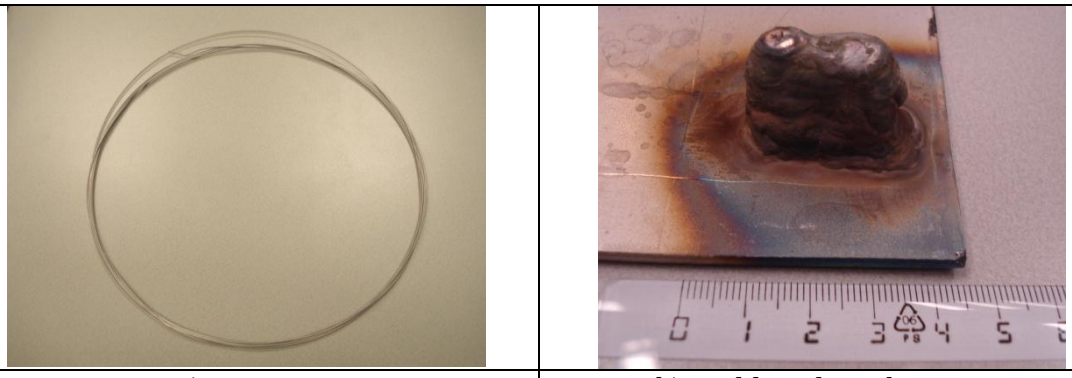

a) Wire 52 | b) Weld made with wire 52

Figure 2. Wire 52 (a) deposited on a plate (b).

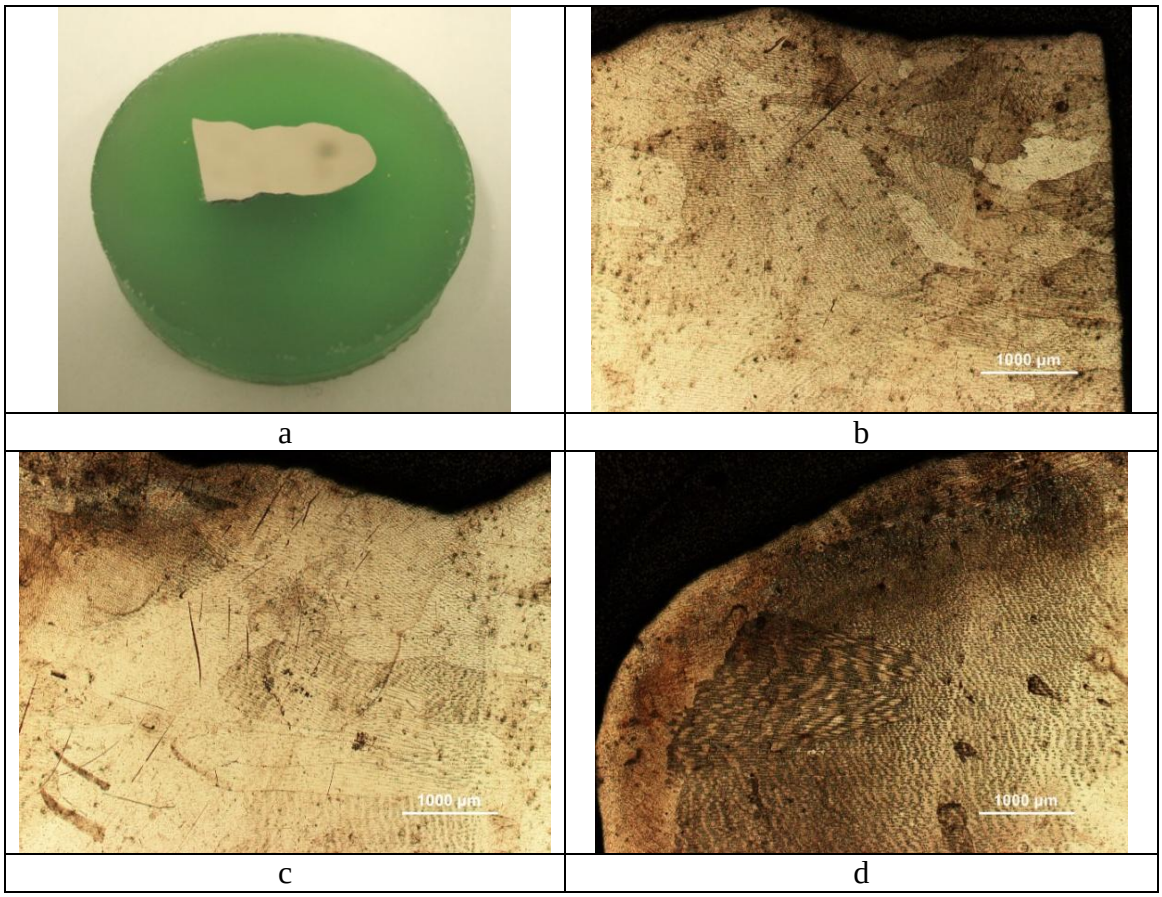

Figure 3. Weld 52 embedded in resin (a) and its microstructure from the lower flat part (b) to the upper round part of the weld (c, d). Etching: Marble solution.

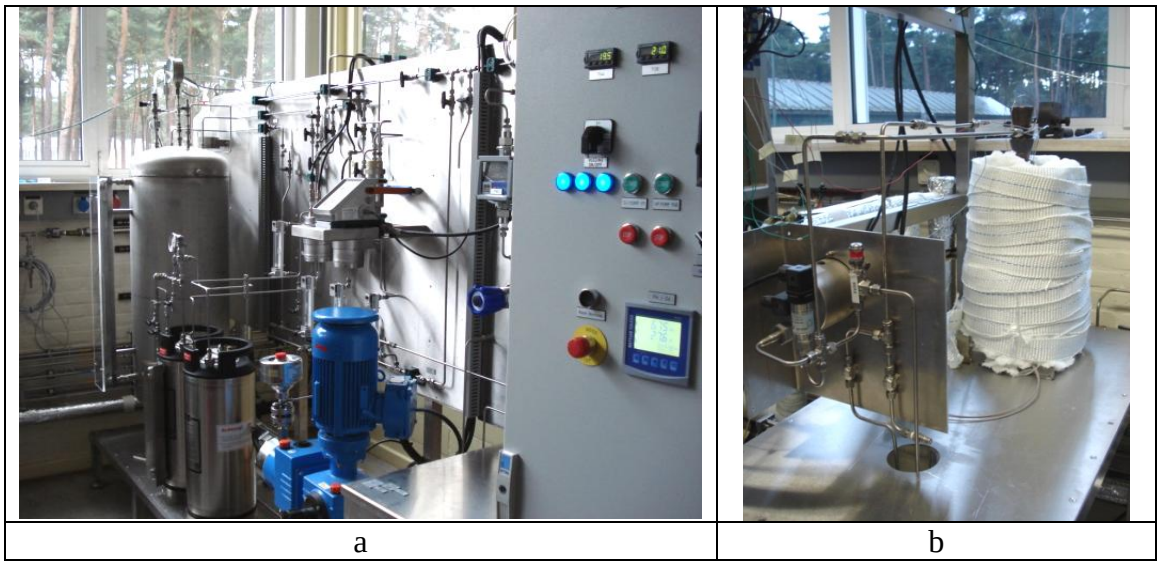

Figure 4. Facility used in the tests. Loop (a); autoclave (b).

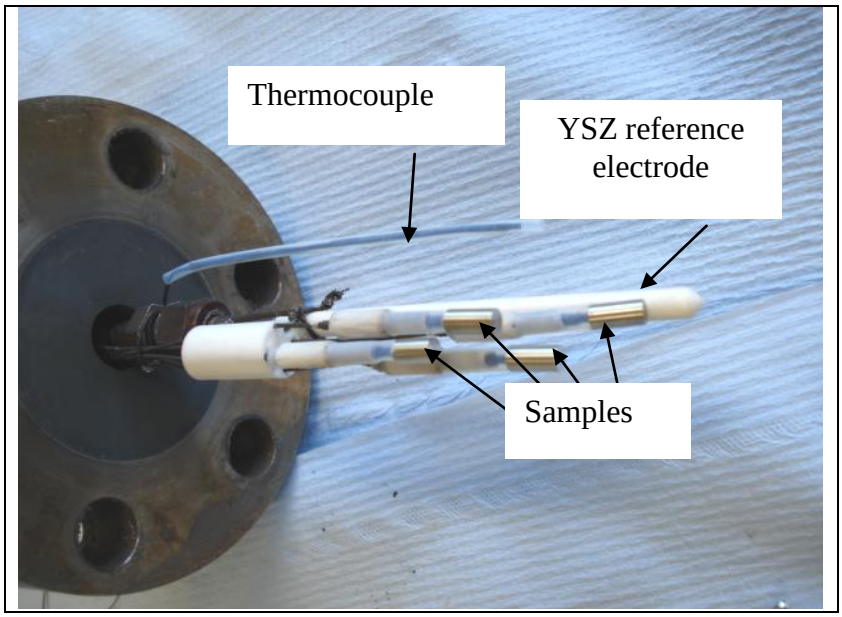

Figure 5. Setup of the specimens installed in the autoclave.

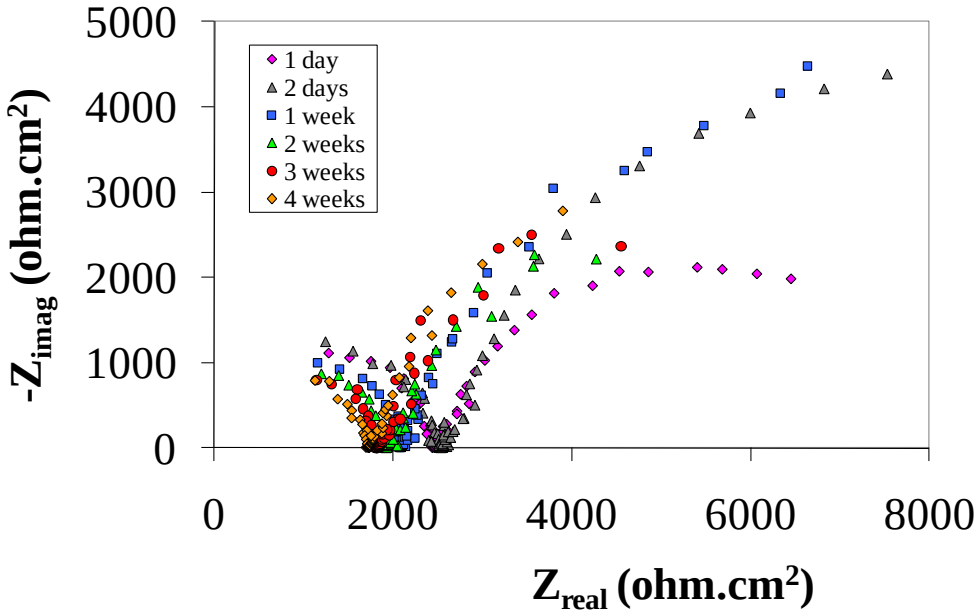

Figure 6. Nyquist plots showing a shift to the left with exposure time for the sample exposed to the condition without hydrogen.

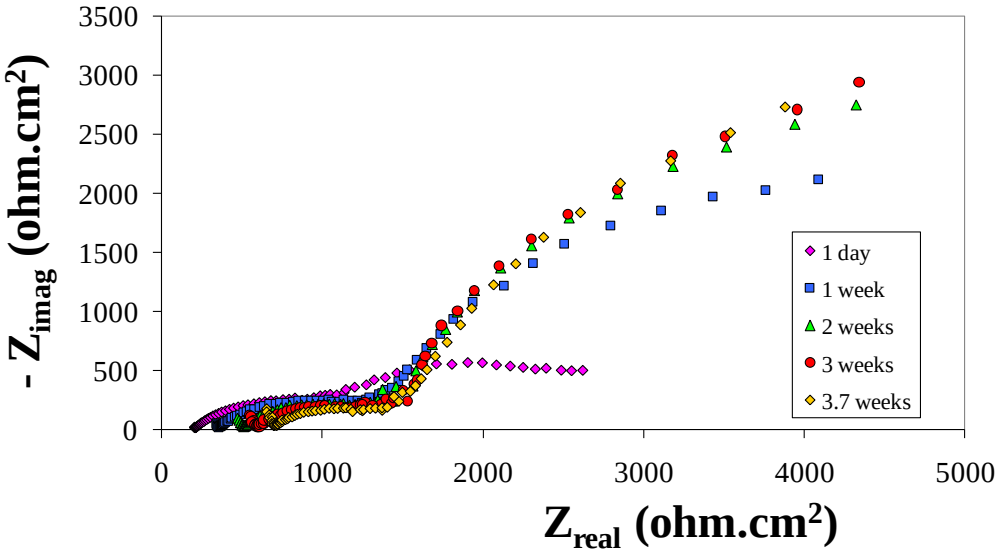

Figure 7. Nyquist plots showing a shift to the right with exposure time for the sample exposed to 25 cm^3/kg H_2.

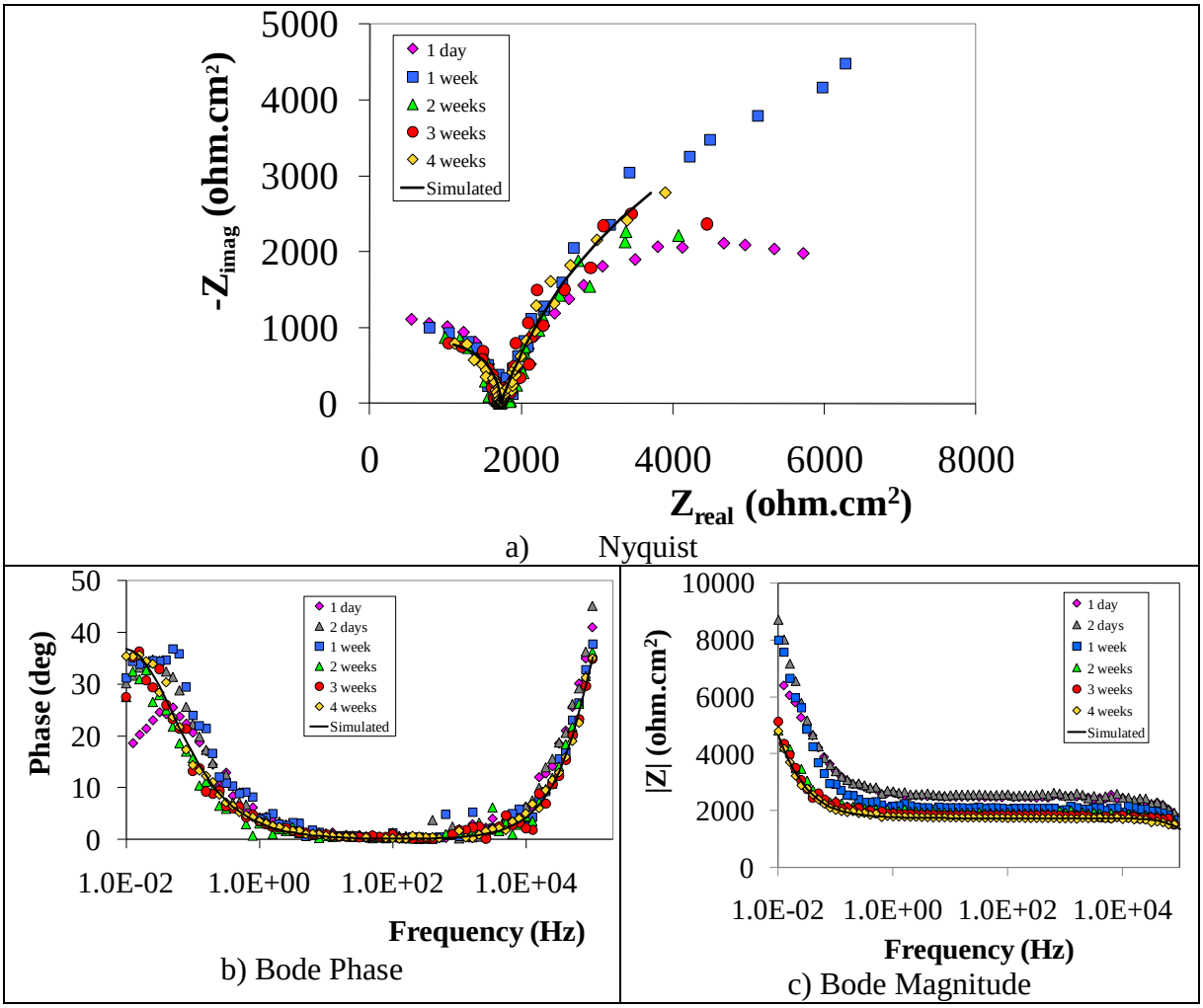

Figure 8. Impedance data for alloy 52 exposed for 4 weeks to PWR water without dissolved hydrogen. The lines represent the result from the equivalent circuit analysis.

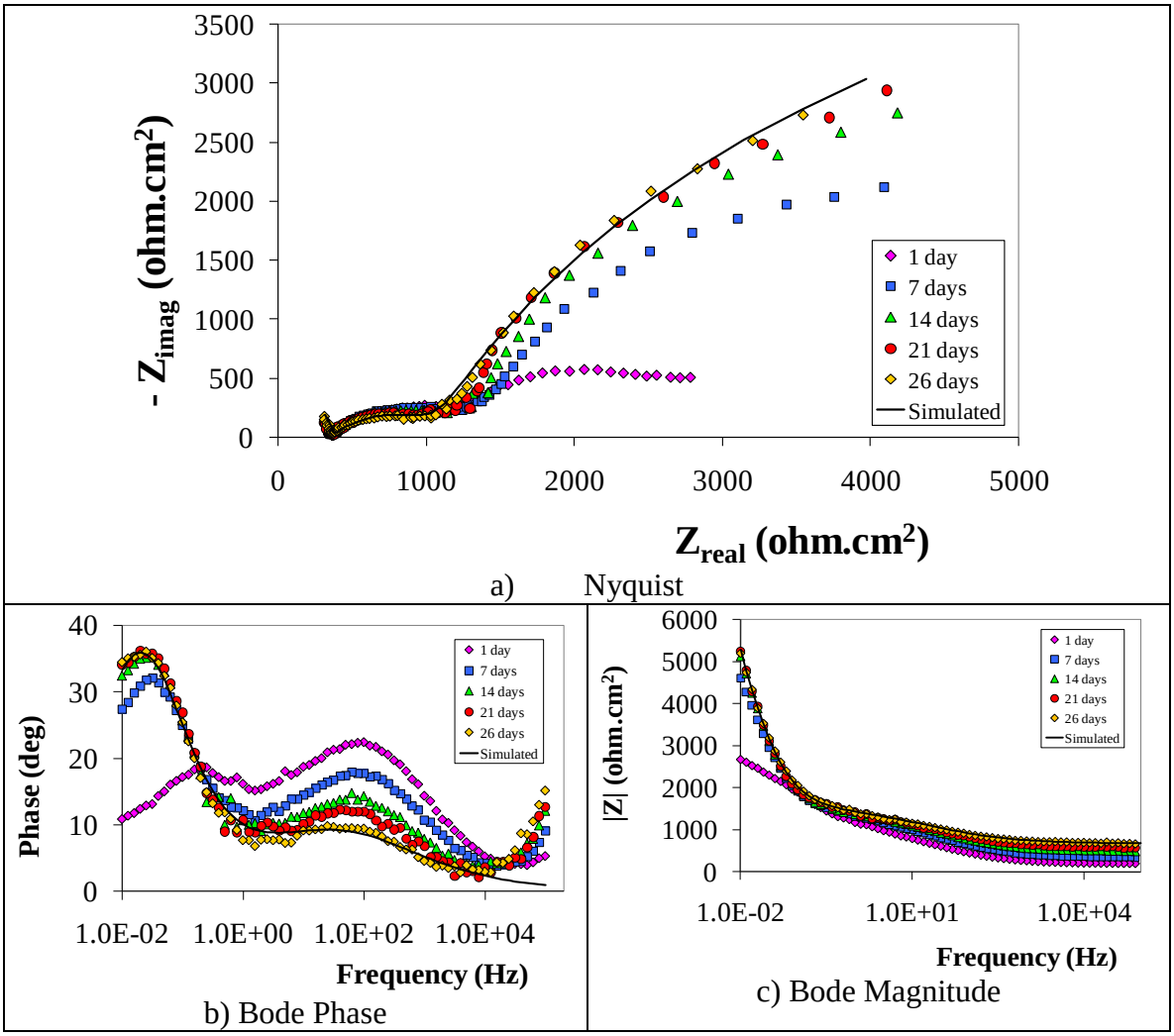

Figure 9. Impedance data for alloy 52 exposed to PWR water with 25 cm^3/kg dissolved hydrogen. The lines represent the result from the equivalent circuit analysis.

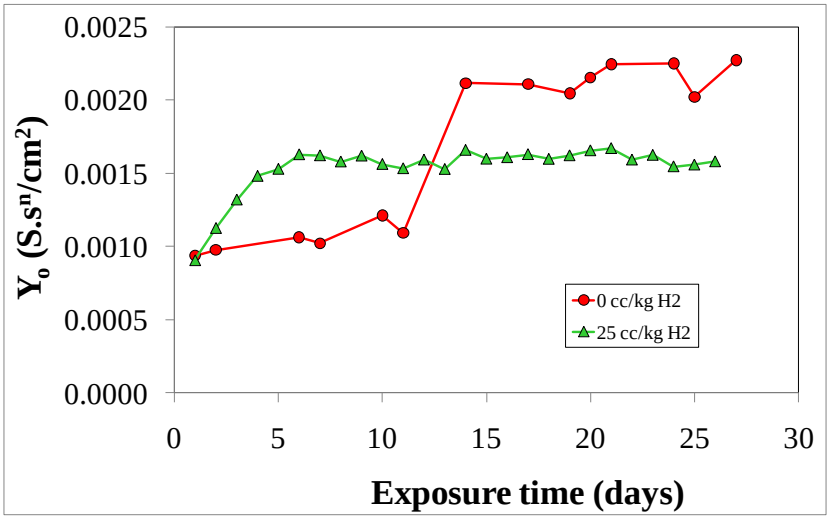

(a)

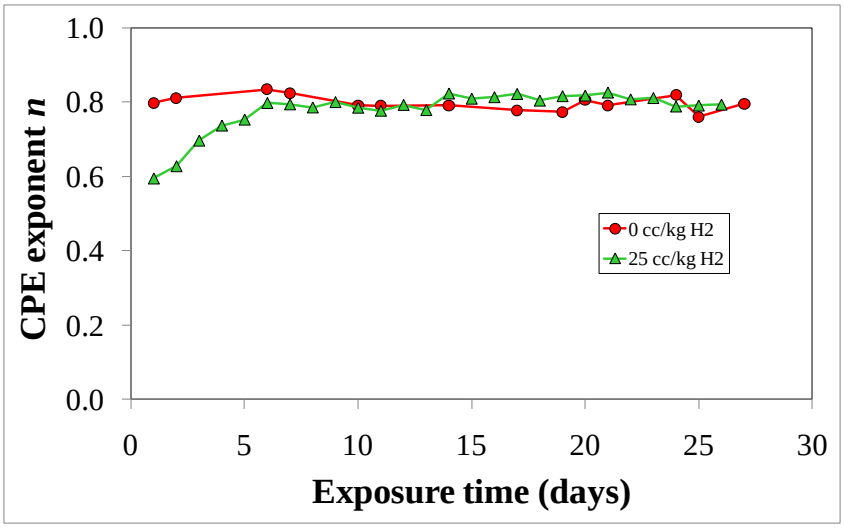

(b)

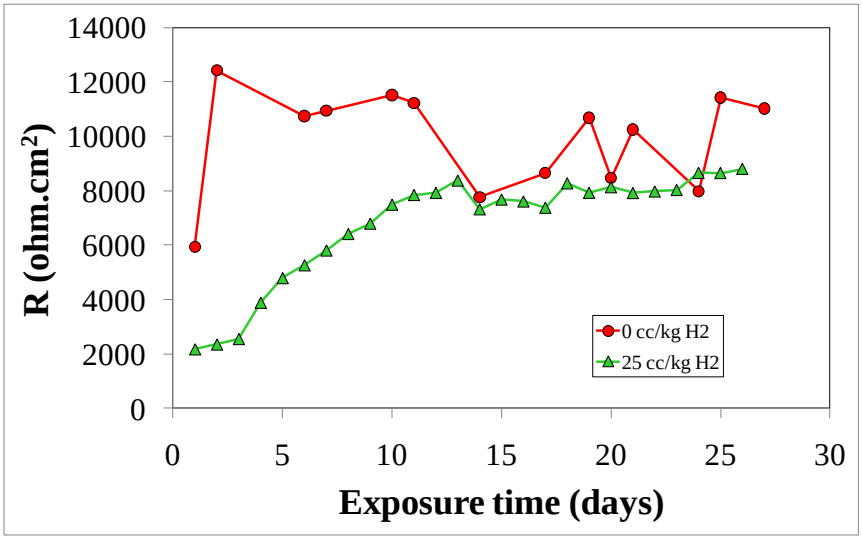

(c)

Figure 10. Evolution of parameters Q_2 and R_2 from the equivalent circuit with exposure time for samples exposed to 0 and 25 cm^3/kg H_2.

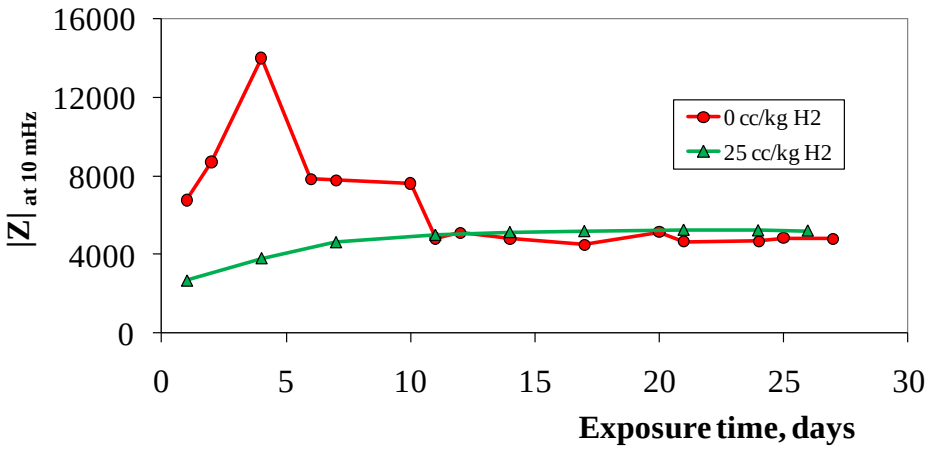

Figure 11. Evolution of experimental impedance data at low frequency (10 mHz) with exposure time for samples exposed to 0 and 25 cm^3cc/kg H_2.

Table 1. Limiting chemical composition of alloy 52 (wt %).

Ni + Co	**Cr**	**Fe**	**C**	**Mn**	**S**	**Ti**	**Si**	**Cu**	**Nb+Ta**
Bal.	28.0-31.5	7-11	≤ 0.04	≤1.0	≤0.015	≤1.0	≤0.50	≤0.30	≤0.10

Table 2. Welding parameters used to deposit the wire 52.

Process	**Electrode size (mm)**	**Current (A)**	**Voltage (V)**	**Travel speed (mm/s)**	**Heat input (kJ/mm)**
GTAW	1.0	90 – 91	12 – 15	4 – 7	0.186 – 0.310